Branched Morphology of Nb powder particles fabricated by calciothermic reduction in $CaCl_2$ melt

Nobuyoshi Suzuki*

Ryosuke O. Suzuki**

Shungo Natsui

Tatsuya Kikuchi

Division of Materials Science and Engineering,

Faculty of Engineering, Hokkaido University,

Kita-13, Nishi-8, Kita-ku, Sapporo, Hokkaido

060-8628, JAPAN

* nbys.suzuki@eng.hokudai.ac.jp

** rsuzuki@eng.hokudai.ac.jp

A new branched morphology of metallic niobium powder particles was produced by calciothermic reduction of niobium oxides in molten $CaCl_2$. The influence of some reaction parameters on the powder particle morphology was studied, and the formation mechanism was investigated. It was found that the formation of intermediate complex niobium oxides ($Ca_xNb_2O_y$) was crucial in the formation of niobium powder particles with the branched morphology. Based on this finding, the formation mechanism of the

branched morphology in four stages was proposed. These Nb powder particles with microscopic branches can prevent particle sintering during the fabrication process of electric capacitors, allowing the latter to exhibit a higher capacitance.

KEYWORDS: Calciothermic reduction; Niobium oxide; Powder morphology; Niobium powder; Molten salt.

1. Introduction

Ta fine powder has been used for high-grade capacitors because the combination of a tantalum oxide film on the surface of a purely metallic bulk gives excellent capacitance and conductivity. Therefore, high-performance Ta capacitors have been primarily utilized in the production of electronic devices commonly found in automobiles, smartphones, personal computers, and gaming consoles. The high conductivity and capacitance of Ta are attributed to a low oxygen concentration in the bulk metal and a large powder surface area. However, Ta powder has become expensive because of the low abundance of its ores, which in turn has raised the price of Ta capacitors. While the market is spurring the development of cheaper electronic devices, responding to the increasing demand of Ta powder has become problematic.

The Nb powder is an alternative to the Ta powder. In the periodic table of elements, Nb lies just above Ta. Consequently, Nb has similar properties as Ta. Notably, Nb oxide exhibits high corrosion resistance because it is a very dense oxide film, similarly to Ta oxide. Additionally, Nb ores are available at a reasonable price [1].

High-purity Nb powder can be produced by the reduction of K_2NbF_7 using liquid

sodium in molten salts [2], or of Nb_2O_5 using magnesium or a mixture of magnesium and hydrogen vapor [3-6]. Because the Ta powder has been produced by the former method, the use of this technology could be easily transferred to the preparation of Nb powder. However, certain operating conditions such as the mass balance among the molten salt, reductant and raw fluoride, stirring during the reaction, and feeding conditions of the raw materials should be optimized to control the particle size distribution and morphology of Nb powder [2,7-9]. The costly optimization of the Nb powder production and the expensive fluoride would therefore not significantly lower the cost of Nb electronic devices. Additionally, the industrial exhaust treatment of fluorine has become difficult due to severe environmental regulations.

The latter method, magnesiothermic reduction, can produce fine Nb particles. However, controlling the grain size distribution and morphology is difficult as well, because the exothermal heat that accompanies the chemical reaction is not sufficiently rapidly released from the reaction field, so sintering of the produced particles locally becomes significant. The replacement of Mg with Ca has been investigated because Ca displays a stronger affinity to oxygen as the reductant and because CaO removal is available [10-17]. In reduction by Ca, the by-product CaO adheres to the formed metal particles as a film, and it is captured among the sintered particles, as in the case of MgO in Mg reduction. These reductant oxide films may become an obstacle to further reduction and deoxidation from the metal particles. On the other hand, it has been reported that the CaO film at the reduction interface can dissolve into molten $CaCl_2$ [18], and that fine Ta and Nb powders can be obtained directly from Ta_2O_5 and Nb_2O_5 [10-17], respectively. Note that these reductants, Mg and Ca, are much cheaper than K_2TaF_7 and K_2NbF_7.

The overall reactions in the calciothermic reduction are:

$Ta_2O_5 + 5\ Ca\ (in\ CaCl_2) \rightarrow 2\ Ta + 5\ CaO\ (in\ CaCl_2)$ (ΔH^0_{1223K} = -1205 kJ/mol [19]), (1)

$Nb_2O_5 + 5\ Ca\ (in\ CaCl_2) \rightarrow 2\ Nb + 5\ CaO\ (in\ CaCl_2)$ (ΔH^0_{1223K} = -1347 kJ/mol [19]). (2)

The reactions (1) and (2) successfully produced fine powders with low oxygen contents and a coral-like morphology [12, 13], which was also seen in the calciothermic reduction of TiO_2 [20, 21], and NiO [22]. This morphology is commonly formed when molten salts are used.

A performance enhancement of Ta capacitors is expected with the use of fine Ta powder as it would increase its capacitance. However, fine particles easily sinter during the manufacturing process, and, as a result, fine grain size cannot be achieved. Baba and Suzuki reported the innovative fabrication of a Ta powder having a broccoli-like particle morphology, obtained by positional exchange between the raw material and reductant during an exothermic reaction [13, 16]. These broccoli-like Ta powder particles can prevent particle sintering and increase the capacitor capacitance when mixed with spherical powder particles. The broccoli branch plays the role of a supporting frame structure during the sintering process into a capacitor pellet [16].

This desirable powder morphology was also obtained for Nb powders using $Nb(OH)_5$ [17] as the raw material. Abnormal morphologies such as bar or slab-like morphologies were obtained, and a higher capacitor's conductivity was obtained by mixing these particles with spherical particles [17]. The reduction of NbO flakes to bar-like Nb particles was also reported [23]. The density difference between NbO and Nb

furthermore generated cracks. By performing reduction followed by deoxidation, Nb with a tree-like morphology was formed. Many of its thin branches remained even after subsequent sintering into a capacitor pellet. These Ta and Nb morphologies were both obtained by thermochemical reduction by reductants; however, the crystalline structure of the raw oxides was different. The stable oxide Ta_2O_5 was used to form broccoli-like Ta, while $Nb(OH)_5$ was applied to form bar-like Nb. The use of the most stable niobium oxide, Nb_2O_5, did not yield such abnormal Nb particle morphology [17]. However, the fabrication of Nb particles directly from Nb_2O_5 would be of significant interest since pretreatment processes such as hydroxide preparation could be avoided, resulting in a reduction in the overall fabrication cost [17].

The purpose of this work is to study the reaction mechanism when Nb_2O_5 is reduced by Ca in molten $CaCl_2$, and to attempt the synthesis of Nb particles with an interesting morphology for the fabrication of high-capacity capacitors.

2.Experimental

2.1 Reduction

The raw materials used were Nb_2O_5 powder (99.9% metallic purity), Ca lumps (a few mm in size, 99.0% metallic purity), and anhydrous $CaCl_2$ powder (99.9% purity). They were filled in a Nb crucible (>99.9% purity, 75 mm internal diameter, 65 mm in depth). The crucible was inserted and sealed in a stainless steel crucible, which in turn was placed in a stainless steel vessel, as shown in Fig.1. The direct measurements of reaction temperature in the vessel was not well worked due to the material reactions with metallic Ca vapor. The temperatures in the stainless vessel were well calibrated with the

external temperature of the furnace.

For production of broccoli-like Ta powder particles, the type of experimental setup was reported to play an important role [13]. Therefore, we examined the influence of four different setups, as shown in Fig.2. In the A-type setup, used for Samples I–V, VI' and VII', both the Ca lumps and Nb_2O_5 powder were placed underneath the $CaCl_2$ powder. At the reaction temperature (1123 K), both Ca and $CaCl_2$ were liquid, while Nb_2O_5 and (newly formed) Nb remained solid. It was reported [13] that the less dense Ca liquid flowed on the denser molten $CaCl_2$, forming a two-layered liquid due to immiscibility of the two liquids at this temperature [18, 24]. The denser Nb_2O_5 powder settled on the bottom of the Nb crucible. Note that Nb metal is the densest. In the B-type setup, the reactants were placed in the crucible in the following order (from bottom to top): Ca lumps, $CaCl_2$ powder, and Nb_2O_5 powder. In the C-type setup, the order was Nb_2O_5 powder, $CaCl_2$ powder, and Ca lumps, while in the D-type setup, it was $CaCl_2$ powder, Nb_2O_5 powder, and Ca lumps. The samples were reacted at 1223 K for 3.6, 7.2, or 14.4 ks in an Ar atmosphere. The Nb_2O_5 powder/Ca reductant/$CaCl_2$ solvent molar ratio was set to 1:2:30 (Sample I), 1:5:80 (II), 1:10:150 (III), 1:20:100 (IV) or 1:30:60 (V).

After reaction, the sample was cooled in Ar gas. The solidified salts and calcium were removed by washing in distilled water. The sample powder was rinsed with distilled water, diluted acetic acid and ethanol. It was then filtered and dried under vacuum.

2.2 Synthesis of complex oxide and reduction

Nb_2O_5 powder and calcined CaO powder (99.9% purity) were mixed and pressed into a disk-shaped pellet with a diameter of 20 mm and a thickness of a few micrometers. These samples were reacted at 1223 K for 3.6 ks in Ar atmosphere to synthesize

complex oxides. The Nb_2O_5 powder/CaO molar ratio was set to 1:1 (Sample VI), 1:10 (Sample VII), 1:1 in $CaCl_2$ (Sample VIII), and 1:10 in $CaCl_2$ (Sample IX).

After reaction, Samples VI and VII containing the newly formed complex oxides were reduced by Ca, and are hereafter referred to as Samples VI' and VII'. The Nb_2O_5/Ca reductant/$CaCl_2$ solvent molar ratio in Samples VI and VII was set to 1:10:150.

2.3 Analysis

The different phases in the samples were identified by X-ray diffraction (XRD) using Cu-Kα ray at room temperature. The morphology of the samples was examined with a scanning electron microscope (SEM), and their composition was determined using an energy dispersive X-ray spectroscope (EDS) equipped with SEM. The oxygen concentration was analyzed by an inert-gas extraction–infrared absorption method using LECO® TC-600.

3. Results and discussion

3.1 Reduced powders

The white particles of Nb_2O_5 exhibited a homogeneous size distribution with a diameter smaller than 1 μm, as is shown in Fig. 3. After reduction and salt separation, a gray powder was obtained in Sample I, while a black powder was obtained in Samples II–V. The XRD measurements at room temperature allowed us to identify metallic Nb in Samples I–V, and NbH in Samples III–V, while complex oxides ($Ca_xNb_2O_y$) were obtained only in Sample I. NbH formed in samples containing more Ca than the stoichiometric ratio with respect to the amount of Nb_2O_5 in Equation 2. We can therefore infer that Ca in excess reacted with the aqueous solution to form H_2 bubbles,

158 which in turn reacted with Nb to form NbH. Therefore, the formation of NbH is
159 associated with the fact that the sample was largely reduced to metallic Nb.

160 SEM images of the obtained powder are shown in Fig. 4. The metallic particles were
161 larger than the raw oxide particles (Fig. 3). Samples III–V displayed a coral-like
162 structure, and a strange branched structure was observed in samples III and IV as well.
163 The diameter and length of these branches were in the range 0.1–1 μm and a few–30 μm,
164 respectively. Sintering between spherical particles and branches was rare in Sample III,
165 while the volume fraction of branches was low in Sample IV. The branched structure
166 looked slightly different from the broccoli-like structure obtained with Ta [12]. On the
167 other hand, some particles with a slab structure were found in Samples I and II, as
168 shown in Fig. 4 (I) and (II). EDS analysis of the samples showed that the slabs were
169 composed of Nb, Ca and O, while the spherical particles in Sample II contained only
170 Nb.

171 Table 1 lists the obtained Nb powder particle morphology alongside the experimental
172 conditions that Samples III were subjected to. A branched morphology was obtained for
173 all the experimental conditions tested. The volume fraction of the branches depended
174 neither on the reaction time nor on the setup types. During the experiment, heavy Nb
175 and Nb_2O_5 might precipitate at the lower parts of melt, and the lighter Ca rose due to the
176 density difference. Regarding setup B, at the beginning of the experiment, there was no
177 physical contact between Nb_2O_5 and Ca, but due to the difference in specific gravity
178 after melting of $CaCl_2$, they may meet only once during the experiment and the
179 thermochemical reduction may progress. However, it should be noted that there was no
180 initial contact in setup C. The reduction had completed although there was no mixing

mechanism such as the difference in specific gravity. In addition, the oxygen concentration of the sample obtained in the setup C was the second lowest value as shown in Table 1. This is because $CaCl_2$ easily dissolves about 5 mol% of Ca at the experimental temperature [24]. Therefore, the dissolved Ca can contact and react with the lower niobium oxides due to fast Ca diffusion, resulting in complete reduction.

The diameter of the spherical particles was generally larger for longer reaction times. However, the length of the branches was hardly affected by the reaction time. This shows that the branched morphology was obtained just after the reduction of the oxide particles.

3.2 Synthesis of complex oxide and its reduction

The synthesis of $CaNb_2O_6$ and $Ca_2Nb_2O_7$ was conducted from the elemental oxides according to the following reactions:

$$Nb_2O_5 + CaO \rightarrow CaNb_2O_6, \quad (3)$$

$$Nb_2O_5 + 2\,CaO \rightarrow Ca_2Nb_2O_7. \quad (4)$$

After reaction without $CaCl_2$, white and hard pellets were obtained (Samples VI and VII), while a white powder was obtained in Samples VIII and IX where CaO was mixed with $CaCl_2$. Fig. 5 shows XRD measurements at room temperature. Complex oxides ($Ca_xNb_2O_y$; with x = 1,2,4 and y = x + 5) were identified in Samples VI–IX. In addition, Nb_2O_5 was identified in Samples VI and VIII.

The Nb_2O_5/CaO molar ratio was set to 1:1 for Samples VI and VIII, but unreacted Nb_2O_5 was still observed after synthesis. CaO was clearly identified in Sample VII,

which can be explained by the low Nb_2O_5/CaO ratio of 1:10. In Sample IX, the same molar Nb_2O_5/CaO ratio was used, but CaO was not detected after synthesis. Because CaO can dissolve in $CaCl_2$ up to 20 mol% at 1223 K [18, 24], unreacted CaO dissolved in $CaCl_2$ melt, and it was thus not identified after reaction. Sample VI did not contain $CaCl_2$, but all of the CaO reacted with Nb_2O_5 to form complex oxides. As can be expected, the complete synthesis with a smaller Nb_2O_5/CaO ratio led to the formation of intermediate oxides with a larger chemical unit, as demonstrates the identification of $Ca_4Nb_2O_9$ in Samples VII and IX. Furthermore, the coexistence of CaO and $CaCl_2$ melt enhanced the formation of $CaNb_2O_6$, $Ca_2Nb_2O_7$ and $Ca_4Nb_2O_9$.

SEM images of Samples VI–IX are shown in Fig.6. Large grains consisting of sub-micron fine particles were formed in Samples VI and VII. Samples VIII and IX exhibited a slab structure similar to that seen in Samples I and II (Fig. 4). This allows us to conclude that complex oxides were formed with a slab morphology when molten $CaCl_2$ coexisted prior to Ca reduction.

After the subsequent reduction of Samples VI and VII by Ca, XRD profiles were measured. They led to the identification of metallic Nb and NbH in both samples (Samples VI’ and VII’). SEM images of Samples VI’ and VII’ are shown in Fig. 7. We could observe that a large number of branches were formed in both samples, with a greater volume fraction of branches in Sample VII’ than in Sample VI’.

3.3 Mechanism of branch growth

As no Nb_2O_5 existed in Sample VII, in contrast to Sample VIII, the larger number of branches in Sample VII’ demonstrates that the branched structure generated from the reduction of intermediate oxides ($Ca_xNb_2O_y$), not of Nb_2O_5. $Ca_xNb_2O_y$ was found to

form with a slab-like or bar-like morphology, as observed in Samples I and II (Fig. 4), and VIII and IX (Fig. 6). The study of the synthesis of $Ca_xNb_2O_y$ showed that the presence of both CaO and $CaCl_2$ melt was required to get this characteristic morphology as it was not obtained in Samples VI and VII.

Therefore, the formation of Nb powder with a branched structure by reduction of Nb-O systems was found to be closely related to the characteristic morphology of $Ca_xNb_2O_y$. Furthermore, even when reducing Nb_2O_5 in the $CaCl_2$ melt, this morphology of complex oxides could be obtained prior to the thermochemical reduction, as in Samples VI and VII (Fig. 6).

Based on our results, we propose the following formation process of Nb branches during the reduction of Nb_2O_5 by Ca.

$$CaNb_2O_6 + 5Ca \rightarrow 2Nb + 6CaO \quad (\Delta H^0_{1223K} = -1211 \text{ kJ/mol [19]}) \tag{5}$$

Initially, CaO is formed as a byproduct of the reaction between Nb_2O_5 and Ca (Reaction (2)). Then CaO reacts with residual Nb_2O_5 powder and forms $Ca_xNb_2O_y$ (Reaction (3,4)) with a bar- or slab-like morphology, as illustrated in Fig.8 (a). Successively, Ca exothermically reacts with $Ca_xNb_2O_y$, to generate metallic Nb and CaO. Heat transmission occurs mainly via conduction along the solid slab. The transmitted heat induces further reduction in a region of the slab close to the first reduction position (Fig. 8(b)). Nb particles are formed and can sinter together into a branch. CaO or CaO-rich $CaCl_2$ liquid coats the surface of the Nb branches, inhibits sintering of the Nb branches with each other (Fig.8 (c)), as has been previously suggested [10-17]. After the removal of solidified salts and residual Ca by water and acid leaching, branched Nb particles are obtained (Fig.8 (d)).

One of the possible reasons why the reaction occurred on the $Ca_xNb_2O_y$ surface is that liquid Ca first spread over and adhered to the reduced Nb particles surface and then diffused to the interface between Nb metal and unreacted $Ca_xNb_2O_y$, i.e. the reaction front (Fig.9 (a)). This explanation may be also apply to $Nb(OH)_5$ [17]. Unfortunately, there is no valid report on the wettability of Ca on the $Ca_xNb_2O_y$ or Nb surface. Considering the strong chemical affinity of Ca with oxides, it is reasonable to assume that Ca easily adheres to oxide surfaces.

In an alternative explanation, however, we may introduce the local contribution of electron transfer during reduction, based on the idea of electronically mediated reaction (EMR) proposed by Okabe et al. [11]: Ca^{2+} and O^{2-} ions originating from the dissolution of CaO in $CaCl_2$ may ensure electron transfer, allowing the reduction of $Ca_xNb_2O_y$ at the three-phase interface (Fig.9 (b)). The reaction with Ca may have occurred on the reduced Nb surface at a separated position from the reduction front, and electrons may have been conducted by Nb metal to the reaction interface. It is not certain whether Ca ions or electrons were transported to the reaction front, but supply of reductants was necessary along the one-dimensional growth direction.

The formation process of Nb branches is certainly slightly different from that of Ta because as reported by previous studies, the Ta branches were formed depending on the spatial setup among the melt, Ta oxide and reductant Ca [13-16]. However, it is noted that there exist several complex oxides in the Ta_2O_5-CaO quasi-binary system. Some previous reports found the existence of complex oxides such as $CaTa_2O_6$ of fibrous structure [25-27]. In particular, the formation of $CaTa_2O_6$ was reported at a relatively low temperature such as 923 K [25]. The enhanced formation of $CaTa_4O_{11}$, $CaTa_2O_6$ and

$Ca_2Ta_2O_7$ was reported in the molten $CaCl_2$ [28,29]. $Ca_4Ta_2O_9$ was also reported in the CaO-Ta_2O_5 phase diagram [30]. Therefore, broccoli-like Ta particles may be formed via a tantalum complex oxide synthesized by a reaction of Ta_2O_5 by CaO. The formation mechanism discussed in this report may thus be generalized to the formation of particles with a branched morphology during calciothermic reduction. Further studies are needed to confirm this hypothesis.

4. Conclusion

Calciothermic reduction of the Nb_2O_5 powder in molten $CaCl_2$ was carried out. The morphology and composition of the obtained products were analyzed by SEM, EDS, and XRD. The formation of Nb powder with a branched morphology, in contrast to spherical particles commonly obtained from oxide powder, was observed. The influence of the reduction conditions such as the $Nb_2O_5/CaCl_2$ molar ratio and the experimental setup on the Nb powder morphology was investigated. We furthermore studied the synthesis of intermediate oxides, and we found out that the formation of $Ca_xNb_2O_y$ with a slab-like morphology was crucial in obtaining the branched morphology. This allowed us to propose the formation mechanism of the Nb powder with branched particle morphology in four stages: (1) formation of CaO from Ca and Nb_2O_5; (2) formation of $Ca_xNb_2O_y$ from CaO and Nb_2O_5; (3) exothermic reaction of Ca with $Ca_xNb_2O_y$; and (4) formation of Nb branches along the $Ca_xNb_2O_y$ longitudinal axis. The branches were coated with CaO, preventing their sintering. Synthesis of $Ca_xNb_2O_y$ prior to performing the calciothermic reduction in molten $CaCl_2$ was furthermore confirmed, and it yielded

294 a larger volume fraction of Nb branches. Therefore, this study paves the way for further
295 improvements of this fabrication method of Nb powder with a characteristic branched
296 morphology, contributing to the fabrication of high-capacitance capacitors.
297

298 ## Acknowledgements

299

300 The authors thank Mr. N. Miyazaki for his assistance on SEM observation and EDS
301 analysis. This work was financially supported in part by JSPS Kakenhi, Grant Number
302 25289267, and by the New Energy and Industrial Technology Development
303 Organization (NEDO) under the “Innovative Pioneering Projects, Number 14100140-b.
304
305

306 # References

307

308 [1] T. Izumi, “Processing of Ta Powder at Cabot-Supermetals Aizu Plant,” Journal of
309 MMIJ (Shigen-to-Sozai), 123 (2007), pp. 711–714.

310 [2] T. Izumi, “Processing of Metallic Material Prospect to the Next Generation. Powder
311 Production Prospect of Tantalum and Niobium,” Kinzoku (Metals Science and
312 Technology) (1999) 69 [10] pp. 875 – 880.

313 [3] L. N. Shekhter, T. B. Tripp, L. L. Lanin, K. Reichert, J. Vieregge, O. Thomas,
314 “Reduction of Nb or Ta oxide powder by a gaseous light metal or a hydride thereof,” US
315 Patent Application PCT Pub. Number WO2000/067936, 5 May 1999.

316 [4] T. Konig, “Process for the Preparation of Finely Divided Metal and Ceramic
317 Powders,” US patent, US 5472477 A, 5 May 1992.

318 [5] I. Park, T. H. Okabe, Y. Waseda, H. S. Yu, O. Y. Lee, “Semi-continuous Production
319 of Niobium Powder by Magnesiothermic Reduction of Nb_2O_5,” Mater. Trans., 42 [5]
320 (2001) pp. 850–855.

321 [6] T. H. Okabe, N. Sato, Y. Mitsuda, S. Ono, “Production of Tantalum Powder by
322 Magnesiothermic Reduction of Feed Preform”, Mater. Trans., 44 [12] (2003) pp. 2646–
323 2653.

324 [7] C. K. Gupta, “Extractive Metallurgy of Niobium, Tantalum, and Vanadium”, Intern.
325 Met. Rev. 29 [6] (1984) pp. 405–444.

326 [8] J.-S. Yoon, S. Goto, B. I. Kim, “Characteristic Variation of Niobium Powder
327 Produced under Various Reduction Temperature and Amount of Reductant Addition,”

328 Mater. Trans., 51 [2] (2010) pp. 354–358.

329 [9] V. N. Kolosov, V. M. Orlov, M. N. Miroshnichenko, T. Yu. Prokhorova, “Preparation
330 of High-purity Tantalum Powders by Sodium Thermal Reduction,” Inorganic Materials,
331 48 [9] (2012) pp. 903-907.

332 [10] R. O. Suzuki, M. Aizawa, K. Ono, “Calcium-deoxidation of Niobium and Titanium
333 in Ca-saturated $CaCl_2$ Molten Salt,” J. Alloy Compd., 288 [1-2] (1999) pp. 173–182.

334 [11] T. H. Okabe, I. Park, K. T. Jacob, Y. Waseda, “Production of Niobium Powder by
335 Electronically Mediated Reaction (EMR) Using Calcium as a Reductant,” J. Alloy.
336 Compd., 288 [1–2] (1999) pp. 200–210.

337 [12] M. Baba, Y. Ono, R. O. Suzuki, "Tantalum and Niobium Powder Preparation from
338 Their Oxides by Calciothermic Reduction in the Molten $CaCl_2$,” J. Phys. Chem. Solids,
339 66 [2–4] (2005) pp. 466–470.

340 [13] R. O. Suzuki, M. Baba, Y. Ono, K. Yamamoto, "Formation of Broccoli-like
341 Morphology of Tantalum Powder", J. Alloy Compd., 389 [1-2] (2005) pp. 310–316.

342 [14] K. Yamamoto, R. O. Suzuki, Y. Ono, M. Baba, "Formation of Broccoli-like
343 Morphology of Ta Powder", in “Molten Salt XIV”, ed. by R. A. Mantz, P. C. Trulove, H.
344 C. DeLong, G. R. Stafford, M. Hagiwara, D. A. Costa, The Electrochemical Society,
345 Penningston, NJ, USA, (2006) pp. 1052–1062.

346 [15] R. O. Suzuki, M. Baba, K. Yamamoto, "Broccoli-like Powder of Ta and Nb by Ca
347 Reduction of Their Oxides", Proc. 7th Int. Symp. on Molten Salts Chem. & Techn.,
348 (29Aug.-02Sept. 2005, Toulouse, France), vol.2, pp. 1063–1066.

349 [16] M. Baba and R. O. Suzuki, "Dielectric Properties of Tantalum Powder with

350 Broccoli-like Morphology", J. Alloys and Comp., 392 [1-2] (2005) pp. 225–230.

351 [17] M. Baba, Tatsuya Kikuchi, R. O. Suzuki, "Niobium Powder Synthesized by
352 Calciothermic Reduction of Niobium Hydroxide for Use in Capacitors", J. Phys. Chem.
353 Solids,78 (2015) pp.101-109.

354 [18] S.Shaw, R.Watson, “Solubility of Calcium in $CaCl_2$ - CaO”, ECS Trans., 16 [49]
355 (2009) pp. 301-308.

356 [19] A. Roine, HSC Chemistry, Ver.6.12, Outokump Research Oy, Pori, Finnland,
357 (2006).

358 [20] R. O. Suzuki and K. Ono "OS Process - A New calciothermic reduction of TiO_2 in
359 the molten $CaCl_2$" Proc. 18th Annual Conf. & Exhibition. of Intern. Titanium Assoc.,
360 (6-8 Oct 2002, Orlando FL, USA) The Intern. Titanium Assoc., Broomfield, CO, USA
361 (2002) "Suzuki_Ono.pdf".

362 [21] T. Abiko, I. Park, T. H. Okabe, "Reduction of Titanium Oxide in Molten Salt
363 Medium", Proceedings of 10th World Conference on Titanium, Ti-2003, [Hamburg,
364 2003. 7. 13-18] (2003) pp.253-260.

365 [22] R. F. Descallar-Arriesgado, N. Kobayashi, T. Kikuchi and R.O.Suzuki,
366 "Calciothermic reduction of NiO by molten salt electrolysis of CaO in $CaCl_2$ melt",
367 Electrochimica Acta, 56 (24) (2011), pp.8422-8429.

368 [23] R. O. Suzuki, I. Ueda, T. Sato, M. Baba and T. Kikuchi, "Reduction of Niobium
369 Oxide Using $CaCl_2$ Melt", Proc. 4th Asian Conference on Molten Salt Chemistry and
370 Technology. Sept.23-27, 2012, Matsushima, Japan, Molten Salt Committee, the
371 Electrochemical Society of Japan. (2012) pp.29-35.

372 [24] K. M. Axler and G. L. DePoorter, “Solubility Studies of the Ca-CaO-$CaCl_2$
373 System”, Materials Science Forum, 73-75, (1991) pp.19-24.

374 [25] L. Janhberg, S. Andersson, A. Magneli, “Polymorphism in Calcium Tantalum(V)
375 Oxide $CaTa_2O_6$”, Acta Chem. Scand. 13 (1959) pp. 1248-1249.

376 [26] L. Janhberg, “Crystal Structure of Orthorhombic $CaTa_2O_6$”, Acta Chem. Scand. 17
377 (1963) pp. 2548-2559.

378 [27] R. M. Almeida, F. M. Matinaga, M. R. B. Andreeta, A. C. Hernandes, A. Dias, and
379 R. L. Moreira, "Polymorphic-Induced Transformations in $CaTa_2O_6$ Single-Crystal
380 Fibers Obtained by Laser-Heated Pedestal Growth", Crystal Growth and Design 13 [12],
381 (2013), 5289-5294

382 [28] R.P. Barnett and D.J. Fray, “Reaction of tantalum oxide with calcium chloride–
383 calcium oxide melts”, J. Mater. Sci., 48 [6] (2013) pp. 2581-2589.

384 [29] R.P. Barnett and D.J. Fray, “Electro-deoxidation of Ta_2O_5 in calcium chloride–
385 calcium oxide melts”, J. Mater. Sci., 49 [12] (2014) pp. 4148-4160.

386 [30] K.T. Jacob and A. Rajput, “Phase relations in the system Ca–Ta–O and
387 thermodynamics of calcium tantalates in relation to calciothermic reduction of Ta_2O_5”, J.
388 Alloy. Compd., 620 (2015) pp.256-262.

Table caption

Table 1 Morphology in the powder obtained at the various experimental conditions when the setup III was taken at 1223 K. The branch structure was commonly observed in the samples III.

Figure captions

Fig. 1 Experimental apparatus.

Fig. 2 Sample filling methods in the crucible.

Fig. 3 SEM image of Nb_2O_5 powder used for reduction.

Fig. 4 SEM images of Nb powder of Samples at setup of I - V.

Fig. 5 XRD profiles of the Samples VI - IX.

Fig. 6 SEM images of the powder in the reduced Samples VI – IX.

Fig. 7 SEM images of Nb powder of VI’ and VII’, which were firstly reacted with CaO without $CaCl_2$.

Fig. 8 Mechanism of branching of niobium. The reduction occurs as (a),(b),(c) and (d) in this turn.

Fig.9 Microscopic mechanism of calciothermic reduction of $Ca_xNb_2O_y$ phase with bar-like morphology. (a) Surface-wetting model and (b) EMR model [11].

409

410

Table 1 Morphology in the powder obtained at the various experimental conditions when the setup III was taken at 1223 K. The branch structure was commonly observed in the samples III.

Time (ks)	Setup	Oxygen (mass ppm)	Morphology
3.6	A-type	7700 ± 200	branch *
7.2	A-type	6900 ± 150	branch
14.4	A-type	5100 ± 100	branch
3.6	B-type	11000 ± 400	branch
3.6	C-type	5800 ± 200	branch
3.6	D-type	6600 ± 150	branch

* shown in Fig.4 (III).

428

429

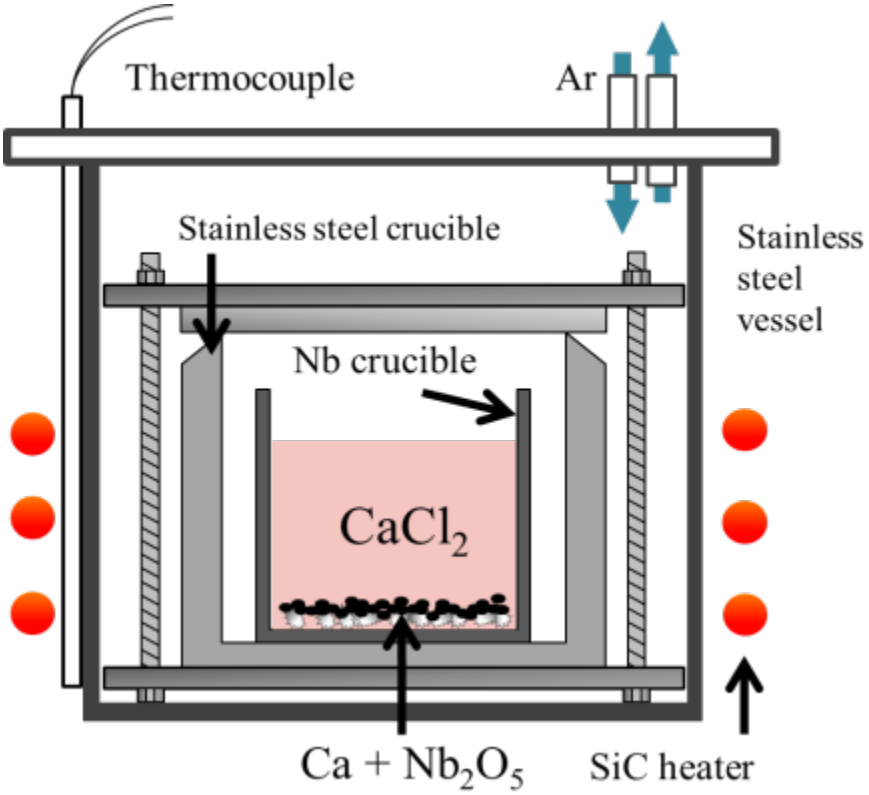

Fig.1 Experimental apparatus.

430

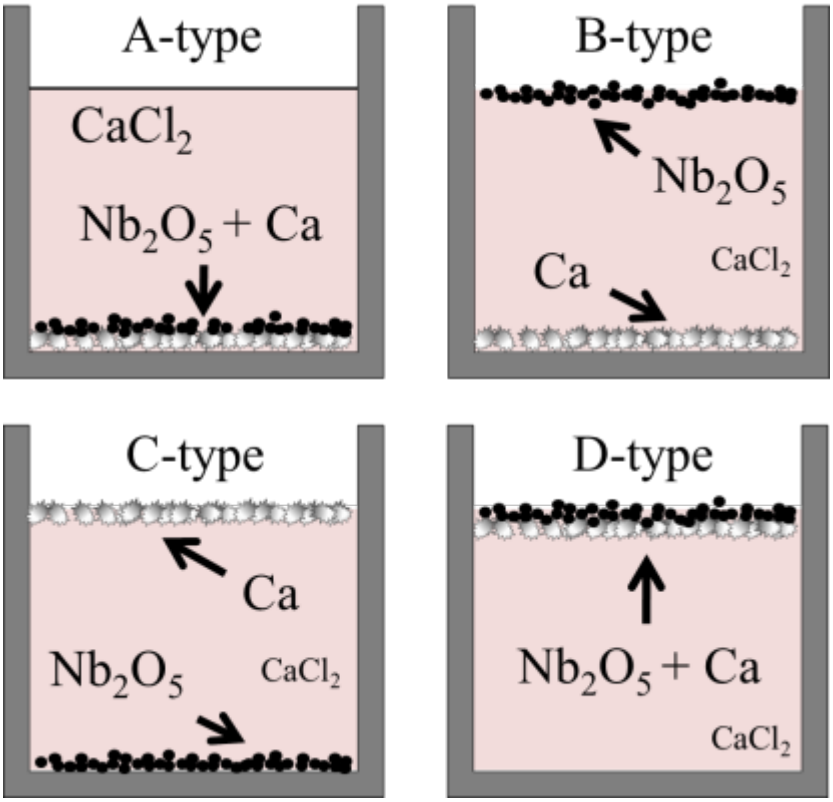

Fig.2 Sample filling methods in the crucible.

431

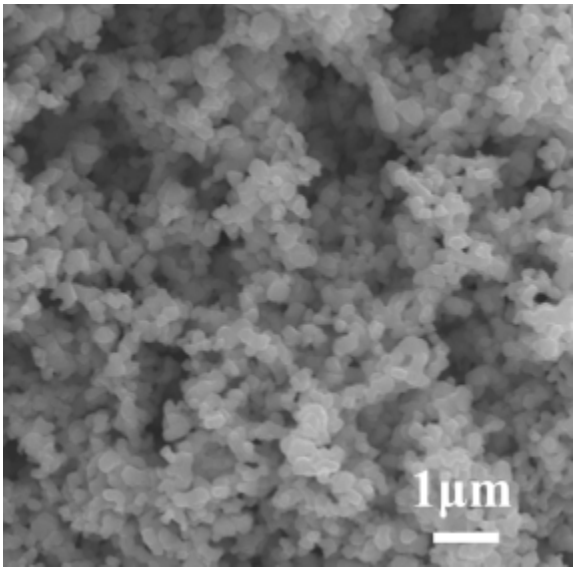

Fig.3 SEM image of Nb_2O_5 powder used for reduction.

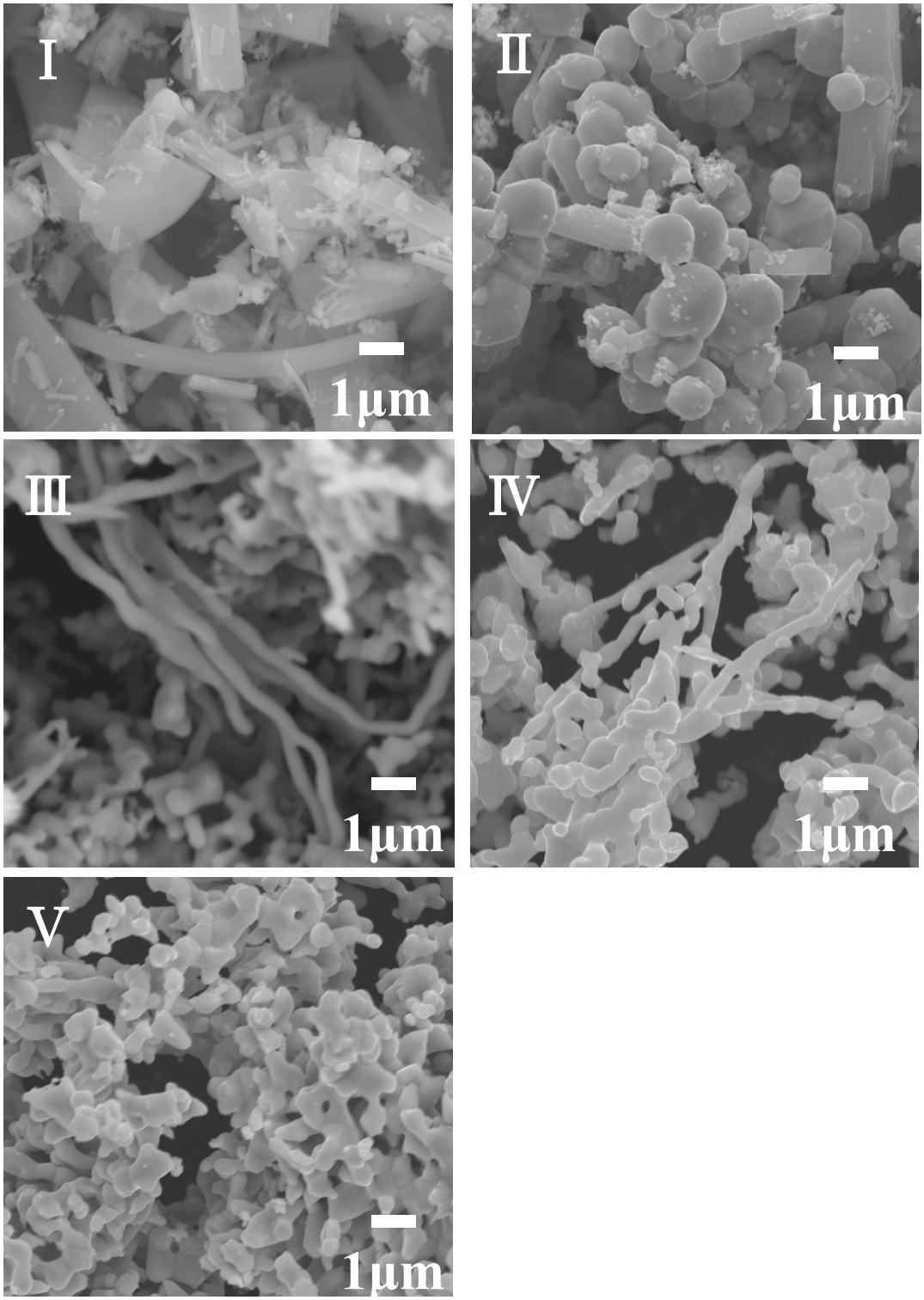

Fig.4 SEM images of Nb powder of Samples at setup of I - V.

433

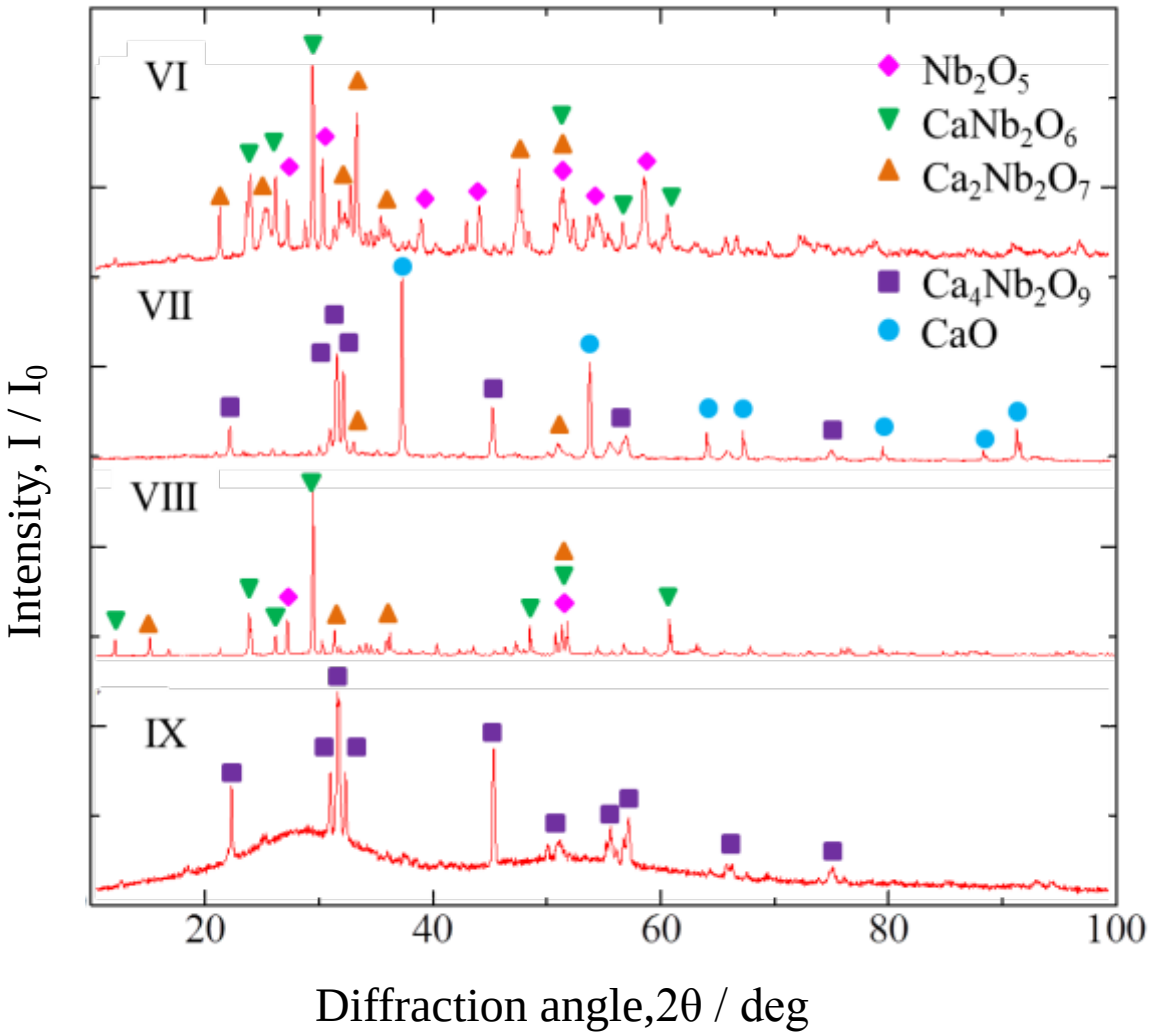

Fig.5 XRD profiles of the Samples VI - IX.

434

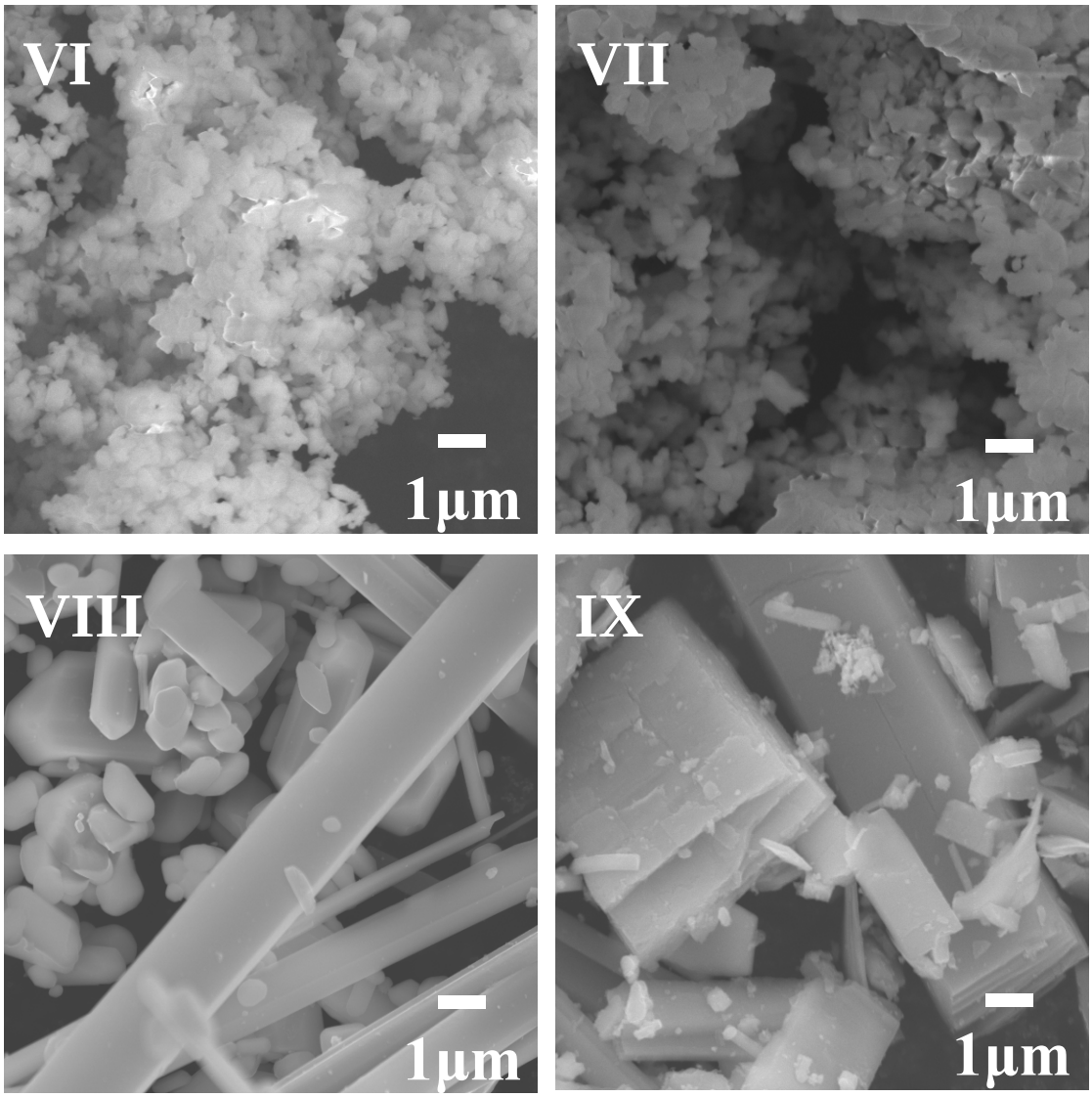

Fig.6 SEM images of the powder in the reduced Samples VI – IX.

435

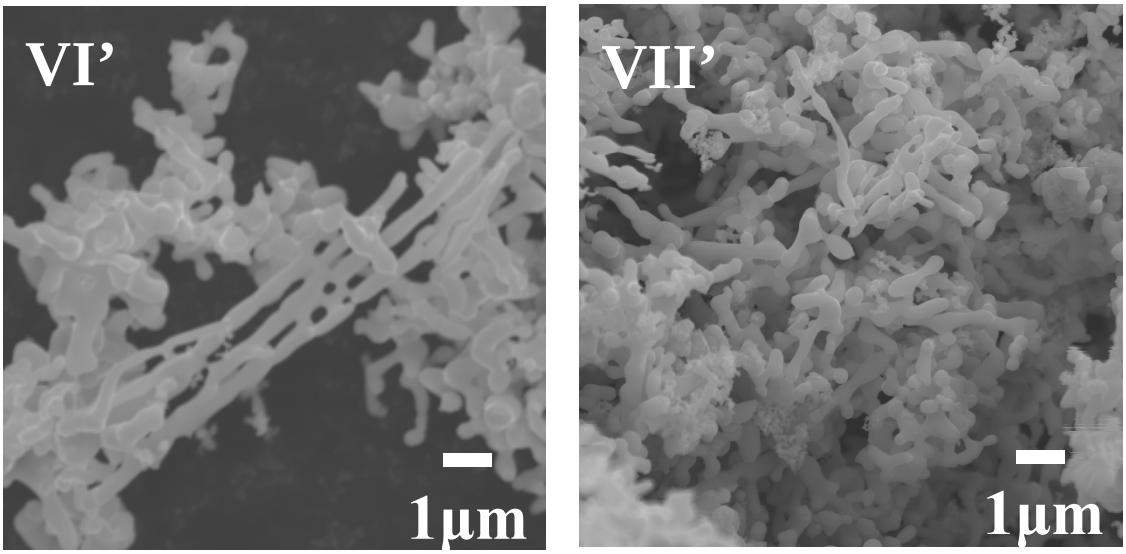

Fig.7 SEM images of Nb powder of VI’ and VII’, which were firstly reacted with CaO without $CaCl_2$.

436

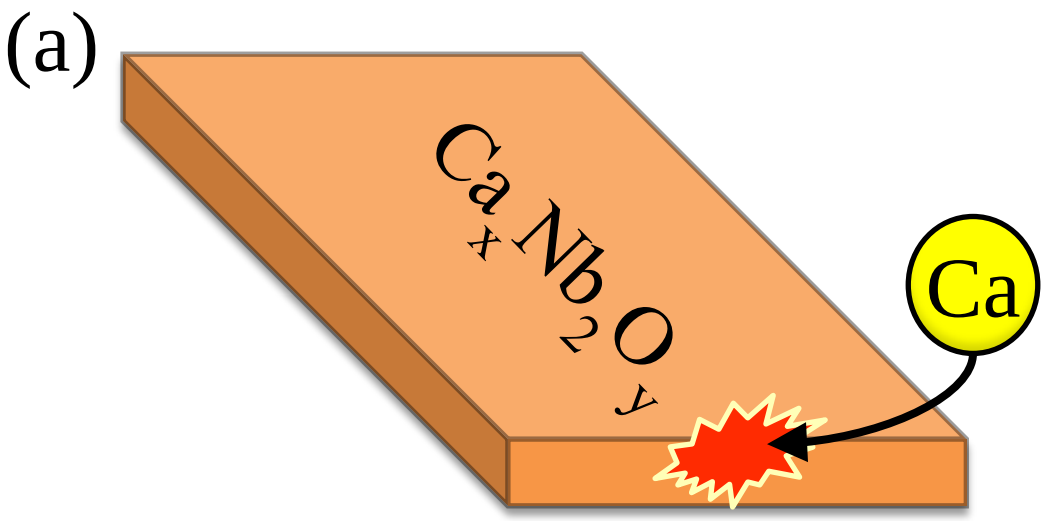

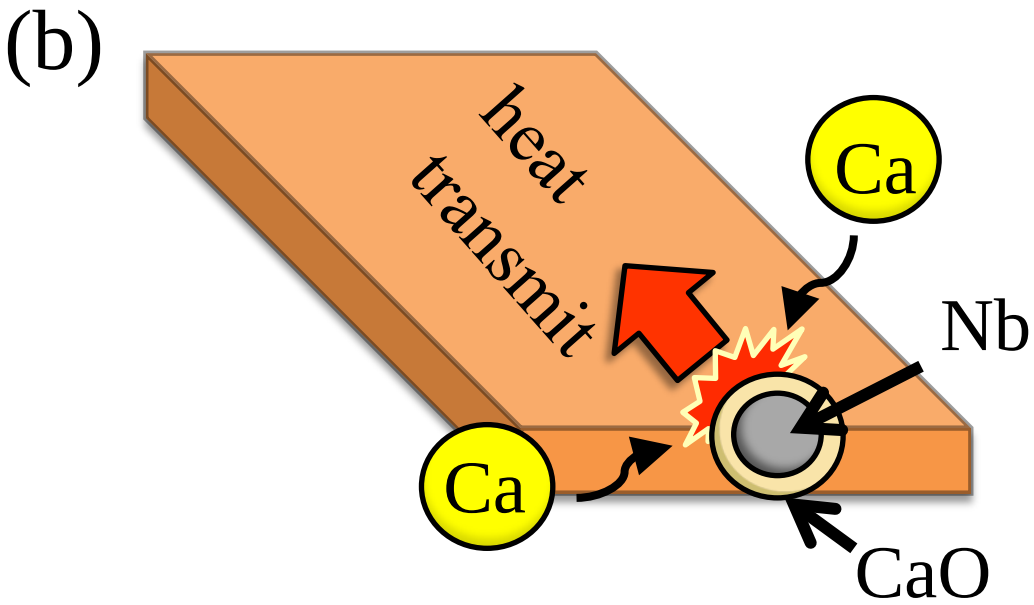

437

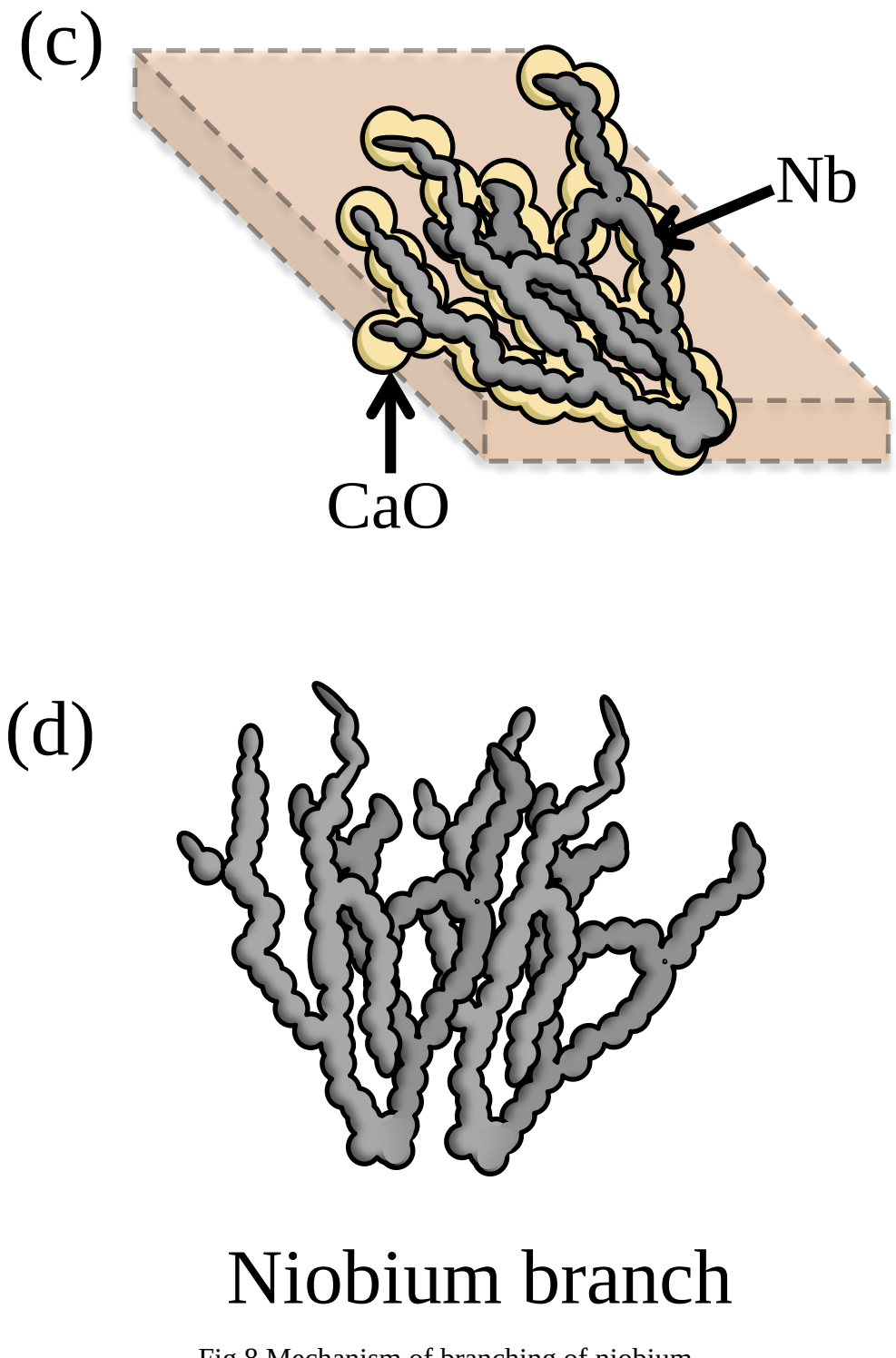

Fig.8 Mechanism of branching of niobium.

The reduction occurs as (a),(b),(c) and (d) in this turn.

438

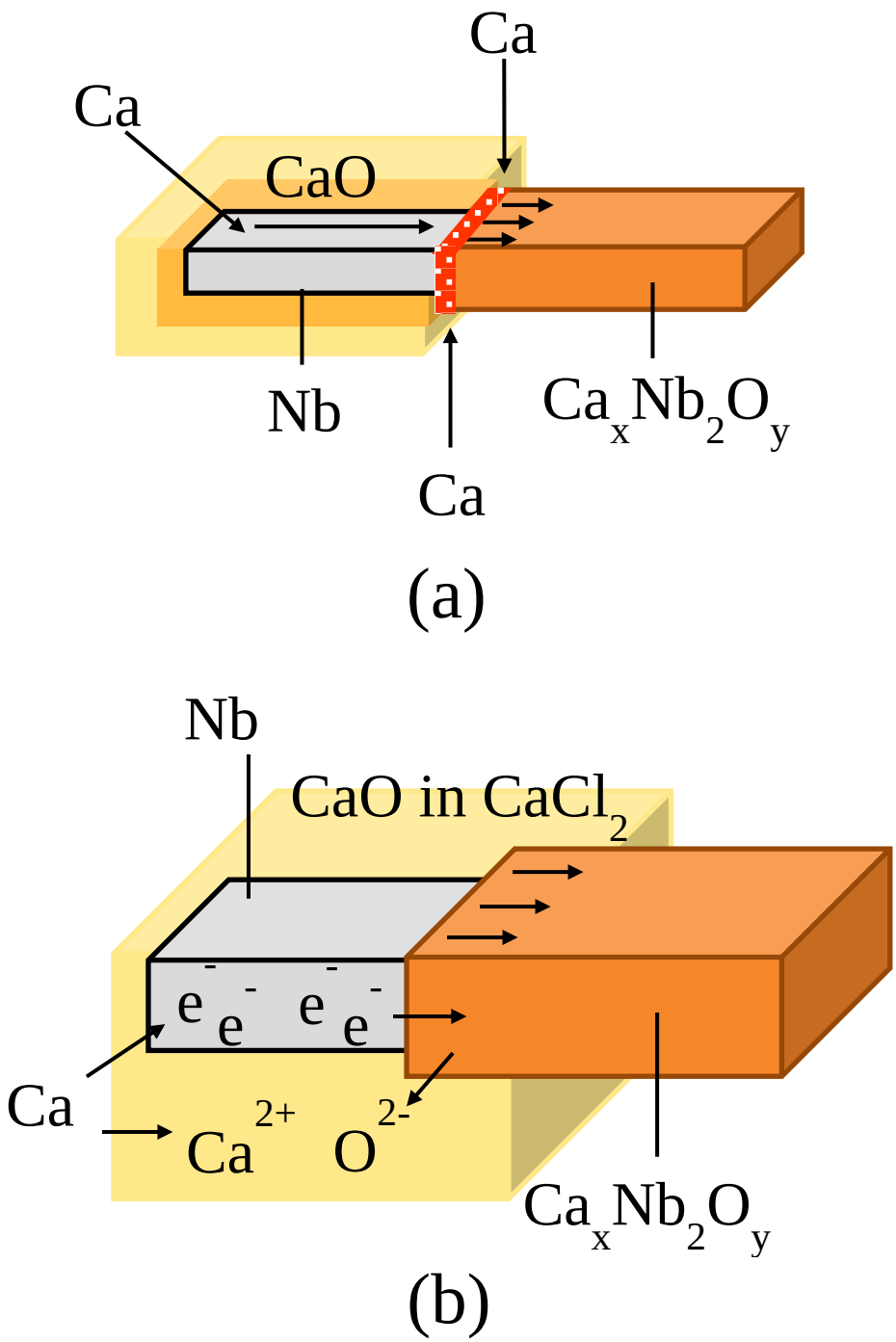

Fig.9 Microscopic mechanism of calciothermic reduction of $Ca_xNb_2O_y$ phase with bar-like morphology. (a) Surface-wetting model and (b) EMR model [11].